Progress In Electromagnetics Research C, Vol. 128, 195–205, 2023

Sixteen-Element Broadband Circularly Polarized Microstrip Antenna Array for S-Band

Mingming Gao, Pengju Yang*, and Jingchang Nan

Abstract—In this paper, a broadband circularly polarized (CP) microstrip antenna array for S-band is proposed. The antenna consists of a parallel rotating feed network, sixteen units with cut corners, adding rectangular perturbations, and the guided patches with 45° oblique rectangular slots. The guided patches increase the impedance bandwidth of the antenna, and the feed network with a 90° phase difference increases the axial ratio bandwidth. The simulation and measurement results show that the S_{11} curve is $2.45 \sim 4.15$ GHz; the impedance bandwidth is 51.5%; the frequency with the axial ratio less than 3 dB is $2.54 \sim 3.74$ GHz; the working bandwidth is 1.2 GHz; the CP bandwidth is 38.2%; the gain is 18.72 dB at the S-band center frequency. The advantages of the designed antenna are high gain, wide bandwidth, and a good radiation pattern. It can be applied to early warning radar in S-band. It also completely covers China Mobile's 2.6 GHz spectrum and can be used as a base station antenna if taking no account of the polarization method. The antenna has a simple structure, which is suitable for applications.

1. INTRODUCTION

The frequency range of the S-band is 2 GHz–4 GHz, which is a short wave, mainly used in the military for medium-distance tracking, monitoring of radar, early warning and alert. In daily life, it is mostly used in Wi-Fi, Bluetooth, and other scenarios. Since the S-band frequency is low, it is easy to achieve a narrow beam width, and the beam width is inversely proportional to the gain. The narrower the beam is, the higher the gain is, which can be used for airport terminal surveillance radar. Therefore, it is of great significance to study the S-band antenna.

The earliest proposed antenna with CP performance is the helical antenna, which was first proposed by Kraus in 1947 [1]. The biggest feature of a helical antenna is that the CP bandwidth is very wide, but its structure is only determined by the angle, not depending on the size, resulting in a negative gain. Used in occasions where only a broad axial ratio bandwidth is required, spiral antenna cannot be widely used. With the efforts of experts and scholars, in 1952, Grieghe and Engelmann defined a new type of transmission line — microstrip transmission line and published related research theories at the same time [2]. In the 1970s, microstrip line was born as a structured microstrip antenna [3, 4]. The structure of the microstrip antenna is simple, and the radiation performance is more prominent than that of the helical antenna. Therefore, later scholars have combined the microstrip antenna with the CP of the antenna, and more CP microstrip antennas with more structures and shapes have emerged. Up to now, although the CP technology of the microstrip antenna has become mature, the CP generated by more structures and methods is still worth learning and exploring.

In recent years, CP antennas are mainly studied in the direction of multi-frequency [5, 6], broad axial ratio bandwidth [7–9], wide beam [10, 11], and high gain [12, 13]. Among them, how to improve the impedance and axial ratio bandwidth of the antenna is a hot research topic at present. Many

Received 12 November 2022, Accepted 28 December 2022, Scheduled 11 January 2023
* Corresponding author: Pengju Yang (1269719753@qq.com).
The authors are with the Liaoning Technical University, China.

researchers have found that a well-performing feed network can greatly improve the impedance and axial-ratio bandwidth of the antenna. For example, in [14], Nasimuddin et al. proposed a patch with a parasitic ring and an "L" shape. The results show that when a continuously rotating 2×2 antenna array is formed, the 3-dB axial ratio bandwidth is 20.6%, and the standing wave bandwidth is 24.0%. Maddio [15] proposed an antenna composed of four slotted disc units and a series feed network structure. The test results show that the 3 dB axial ratio bandwidth is 15.5%; the range is 5.32 GHz $\sim$ 6.22 GHz; the impedance bandwidth is 5 GHz $\sim$ 6.8 GHz (29%); and the peak gain is 8.25 dB. Ta and Park [16] proposed a compact broadband CP antenna array, which is a set of 2×2 metasurface-based CP patch antennas, and the periodic metal plate lattice consists of truncated corner square patches between the ground plane and the metasurface. The results show a 3 dB axial ratio bandwidth of 4.75 $\sim$ 7.25 GHz (41.67%), 3 dB gain bandwidth of 4.8 $\sim$ 7.0 GHz (37.3%), and peak gain of 12.08 dB at 6.0 GHz. The standing wave bandwidth of the antenna is 4.40 $\sim$ 8.00 GHz (58.06%).

In this paper, a CP microstrip antenna array for S-band is proposed. Every unit adopts a simple corner cut and disturbance structure, and the feed network adopts an equalized T-type power divider. The guided patches are with 45° rectangular slots. After simulation and actual measurement, the radiation pattern of the antenna is stable; the impedance bandwidth is 2.45 $\sim$ 4.15 GHz; the frequency with the axial ratio less than 3 dB is 2.54 $\sim$ 3.74 GHz; and the maximum gain reaches 18.72 dB. The antenna with a simple structure is suitable for practical applications.

2. DESIGN OF THE ANTENNA

2.1. Design of the Unit

Unit patch design uses a chamfered patch, and a perturbation rectangle is added above the patch to generate a symmetrical impedance bandwidth. The chamfer improves the impedance bandwidth and also affects the axial ratio. The dielectric substrate is an F4B substrate with a dielectric constant of 2.65 and a thickness of 3 mm. The height of the two-layer dielectric substrate is h_1. Figure 1 shows the structure of the unit.

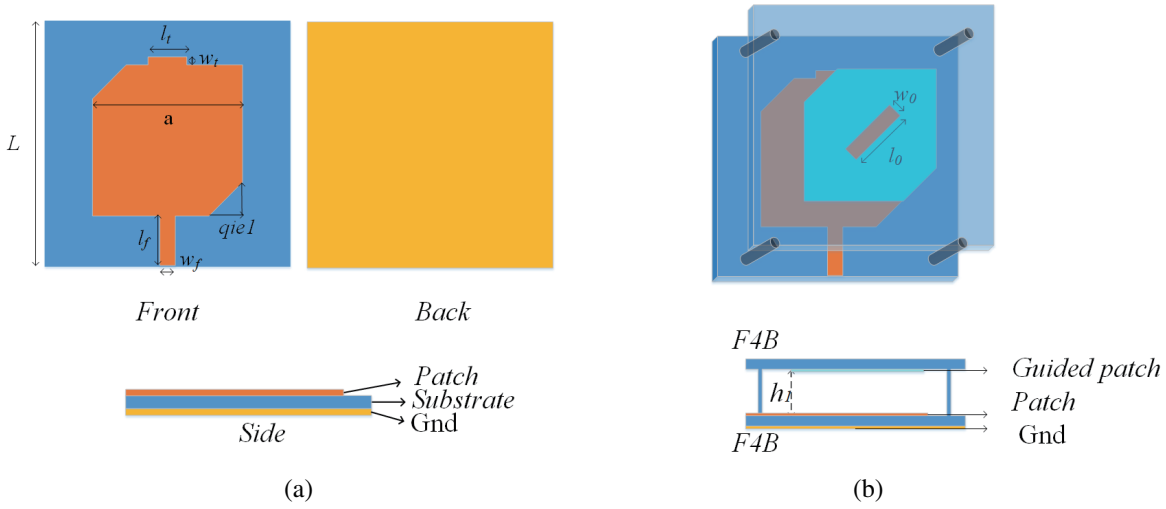

Figure 1. Structure of the unit.

The designed patch antenna works on 3 GHz, which is the center frequency of the S-band. The patch is square, and its length and width dimension formulas are as follows (1)–(4).

$$w_{patch} = \frac{c}{2f}\sqrt{\frac{2}{\varepsilon 0 + 1}} \tag{1}$$

$$l_{patch} = \frac{c}{2f\sqrt{\varepsilon_e}} - 2\Delta l \tag{2}$$

$$\varepsilon_e = \frac{\varepsilon_0 + 1}{2} + \frac{\varepsilon_0 - 1}{2}\left(\sqrt{\frac{w_{p_{atch}}}{12h + w_{p_{atch}}}}\right) \tag{3}$$

$$\Delta l = 0.412h\frac{(\varepsilon_e + 0.3)(w_{patch}/h + 0.264)}{(\varepsilon_e - 0.258)(w_{patch}/h + 0.8)} \tag{4}$$

In the equations [20], w_{patch} and l_{patch} are the length and width of the patch, respectively; ε_0 is the relative permittivity; ε_e is the effective dielectric constant; and Δl is the corrected length. w_{patch} calculated by the above equation is 37 mm; ε_e is 2.41; and Δl is 1.49 mm, resulting in a l_{patch} of 29.23 mm. After optimization, the optimal solution of the cell length and width is 28.7, and a rectangular bar is added above to adjust the shape of the S_{11} curve. The size of the cut angle can make the curve produce a "w" shape so that the bandwidth will be slightly broadened. Figure 2 shows the two different shapes of S_{11} curve.

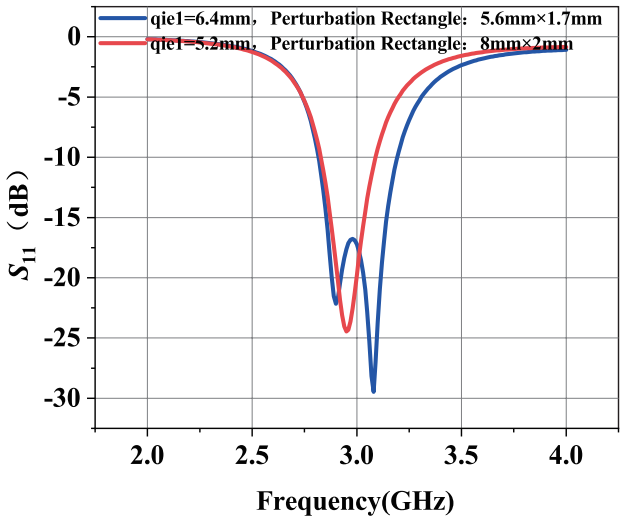

Figure 2. S_{11} curves of different sizes of tangent angle and perturbation structure.

2.2. Design of Power Divider

In practical engineering applications, microstrip antenna often radiates after multiple units are superimposed in an array. How to distribute the power of these units to a certain proportion requires the use of a power divider. Therefore, the power divider is used in the design of the feed network. In general, the power of the signal source can be equally or unequally distributed to each branch. The commonly used power dividers mainly include T-shaped power dividers, microstrip line power dividers, and Wilkinson power dividers. This paper adopts a T-type power divider, from a 2-way power divider to a 4-way power divider with a phase difference, and finally designs a 16-way power divider on the basis of a 4-way power divider. The 4-way power divider is shown in Figure 3.

Since CP waves are to be generated, the four ports need to be phase-shifted during design. According to the principle of CP waves, each port needs to have a phase difference of 90 degrees. The working principle is to feed power from the coaxial, and then the current is divided into two paths. One part is to the left, and the other part is down. The current going down passes through port 2 and port 5, and port 2 is 90 degrees behind port 5, converted to a microstrip line length about a quarter wavelength. The leftward current has a longer path than the downward current. The length is lambda 1, which is about half the wavelength. Then, the phase of port 3 is 90 degrees behind that of port 4. The clockwise lag of 90 degrees from port 5 to port 3 provides conditions for the generation of CP.

Figure 4 shows the output power ratio of the four ports of the power divider. Because it is an equal power divider, the power ratio is 1 : 1 : 1 : 1 in the case of four ports, and each port is about −6 dB.

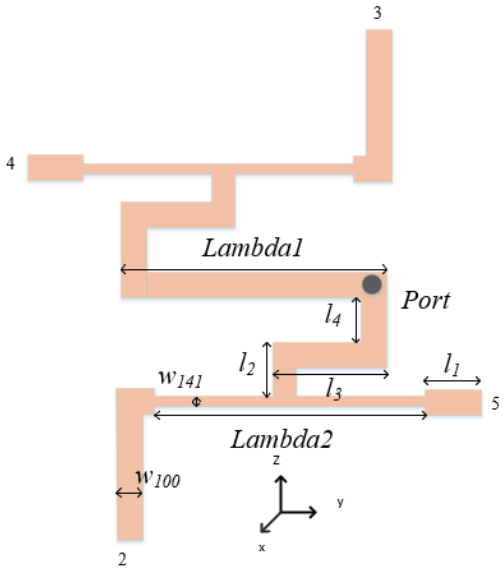

Figure 3. 4-way power divider.

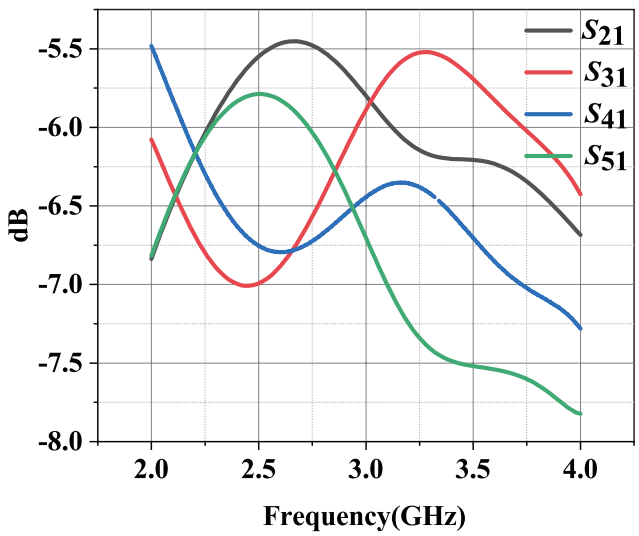

Figure 4. Parameters of power divider $S_{21} \sim S_{51}$.

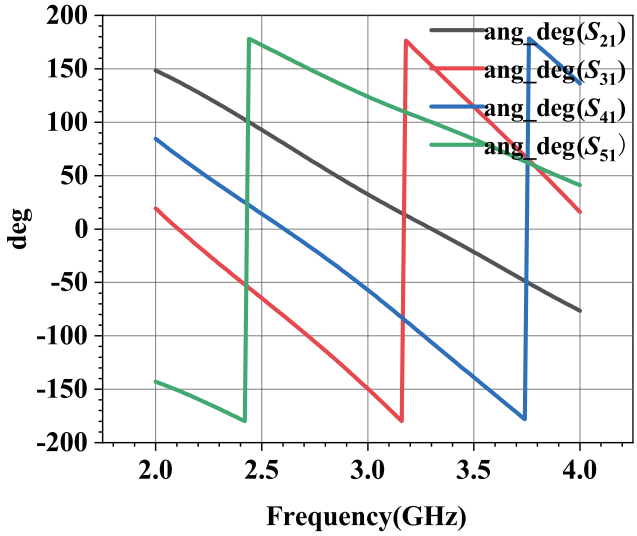

Figure 5. The phase difference of power divider.

Taking into account the loss of the power divider, it is generally enough that the fluctuation does not exceed 1 dB. In the figure, the fluctuation is about 0.8 dB up and down at 3 GHz, which achieves a good effect.

When CP is designed, it is very important to observe the phases of the four ports. If the phase difference cannot be around 90 degrees, the effect of CP will be worse. As can be seen from Figure 5, at 2.5 $\sim$ 3.2 GHz, the phase difference is 90 degrees. As the frequency decreases or increases, the corresponding wavelength is no longer a quarter wavelength. Therefore, it is sufficient to meet the requirements around the center frequency of the solution.

2.3. Sixteen-element CP Antenna Array

The above section introduces the design of the unit patch and power divider. The following is the design of the CP antenna array. There are many advantages of CP antenna array, and one of the most

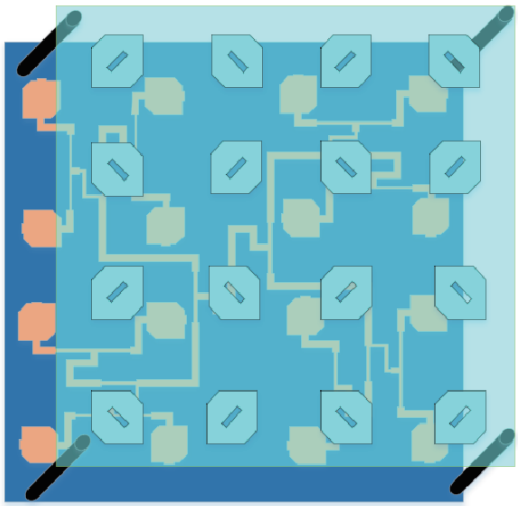

Figure 6. Sixteen-element CP microstrip antenna array.

important is high gain. According to experience, the general gain of a single unit patch is $5 \sim 7$ dB, and the gain is increased by 3 dB every time the number of units increases by a power series of 2. The gain of the 16-element array is generally about $17 \sim 19$ dB. The overall model of the antenna is shown in Figure 6:

The size of the sixteen-element CP antenna array is 258 mm × 258 mm × 3 mm. The final parameters of the unit and power divider in this paper are shown in Table 1.

Table 1. The parameters of the unit and power divider.

parameters	value/mm	parameters	value/mm
a	28.7	l_1	7.4
l_t	5.6	l_2	6
w_t	1.7	l_3	9.6
l_f	8	l_4	4.65
w_f	2.26	w_{100}	2.26
l_0	6	w_{141}	0.85
w_0	1.6	$\lambda 1$	40.22
$qie1$	6.4	$\lambda 2$	34.7
h_1	7	L	50

After introducing 45° rectangular slots in the guided patches, the impedance and axial ratio bandwidth of the antenna are obviously different. Figure 7 compares the S_{11} curve and axial ratio before and after the slot is introduced. It can be seen that the effect of S_{11} and axial ratio has become better. The S_{11} curve is $2.45 \sim 4.15$ GHz; the impedance bandwidth is 51.5 %; the frequency with the axial ratio less than 3 dB is $2.54 \sim 3.74$ GHz; the working bandwidth is 1.2 GHz; the CP bandwidth is 38.2%, an increase of nearly 15%. Therefore, it is of great significance to perform gap processing on the guided patches.

In order to observe the radiation characteristics of the antenna, select three different frequency points (2.7, 3, 3.3 GHz) in the axial ratio bandwidth to view radiation characteristics of the antenna, and the significance of taking three points is to prevent the wrong judgment caused by the sudden change of the direction map. The six graphs in Figure 8 are the polarization directions of the xoz plane

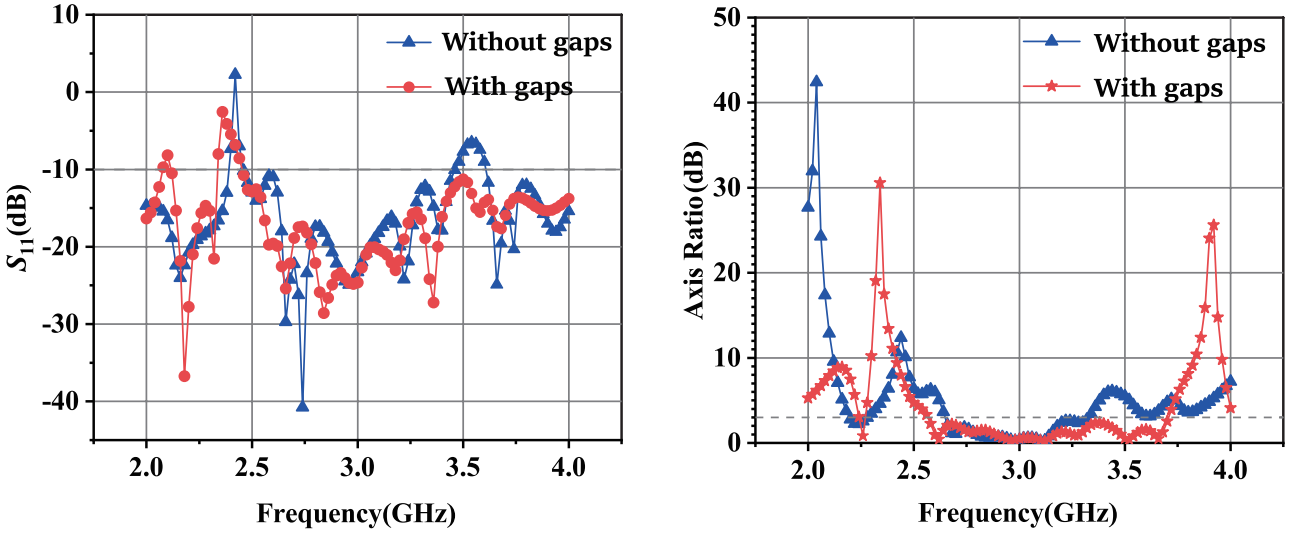

Figure 7. Antenna parameters before and after the introduction of the slit in the leading patch.

and *yoz* plane corresponding to three frequency points from low frequency to high frequency. It can be seen from the six pictures that the polarization modes are all left-handed CP; the radiation of the antenna is the strongest in the direction of 0 degrees; and the backward radiation of the antenna is very small. The cross-polarization isolation is greater than 40 dB. Among them, at 3 GHz, the back lobe of the pattern is smaller; the front-to-back ratio will be relatively larger; and the symmetry is better, so the CP performance is also the best, and each pattern is not off-center.

Figure 9 shows the gain of the three frequency points. It can be seen from the figure that the gain is the largest at 3 GHz, which is 18.72 dB. The gain drops to 16 dB at 2.7 GHz and 3 GHz. The influence of side lobes is not considered in the design; therefore, the overall side lobes are relatively high, whose level is about -14 dB or more.

3. SIMULATION AND MEASUREMENT OF ANTENNA

In order to test the performance of the CP array antenna in the rotary feeding mode, the sixteen-element antenna array was fabricated and passed the parameter test.

The S-parameters were tested using a vector network analyzer, and the pattern and antenna gain were tested in a dark room. The dielectric substrate is F4B with a dielectric constant of 2.65. The joint material is RT5880 with a dielectric constant of 2.2 Rogers, and the size is 3 mm. Figure 10 is a physical map of the antenna.

The simulation and measurement results are shown in Figure 11. The left figure is S_{11} of the antenna, and the right figure is the axis ratio. The range of S_{11} is $2.45 \sim 4.15$ GHz, and the frequency with the axial ratio less than 3 dB is $2.54 \sim 3.74$ GHz. Figure 12 shows the gain of the antenna within the operating frequency. The gain is the highest at around 3 GHz, and then the gain is greater than 15 dB in the range where the axial ratio bandwidth is satisfied, which is basically stable. Figure 13 is the simulation and actual measurement of the antenna pattern at 3 GHz. The radiation of the antenna is the strongest in the direction of 0 degrees, and the backward radiation of the antenna is very small. At 3 GHz the pattern is symmetric with no offsets. The beam width of the pattern can also be seen in the figure. When the gain is decreased by 3 dB, the pattern is about 15 dB scan range. Overall, the beam width is around 20°.

Table 2 shows the comparison between the CP antenna array designed in this paper and the antennas in the published literature. The impedance bandwidth and axial ratio bandwidth have obvious advantages, and the gain is much higher than that of [14, 15, 21, 23]. Compared with [18], the gain is slightly smaller, because its frequency is in the millimeter wave band, and the use of the integrated wave

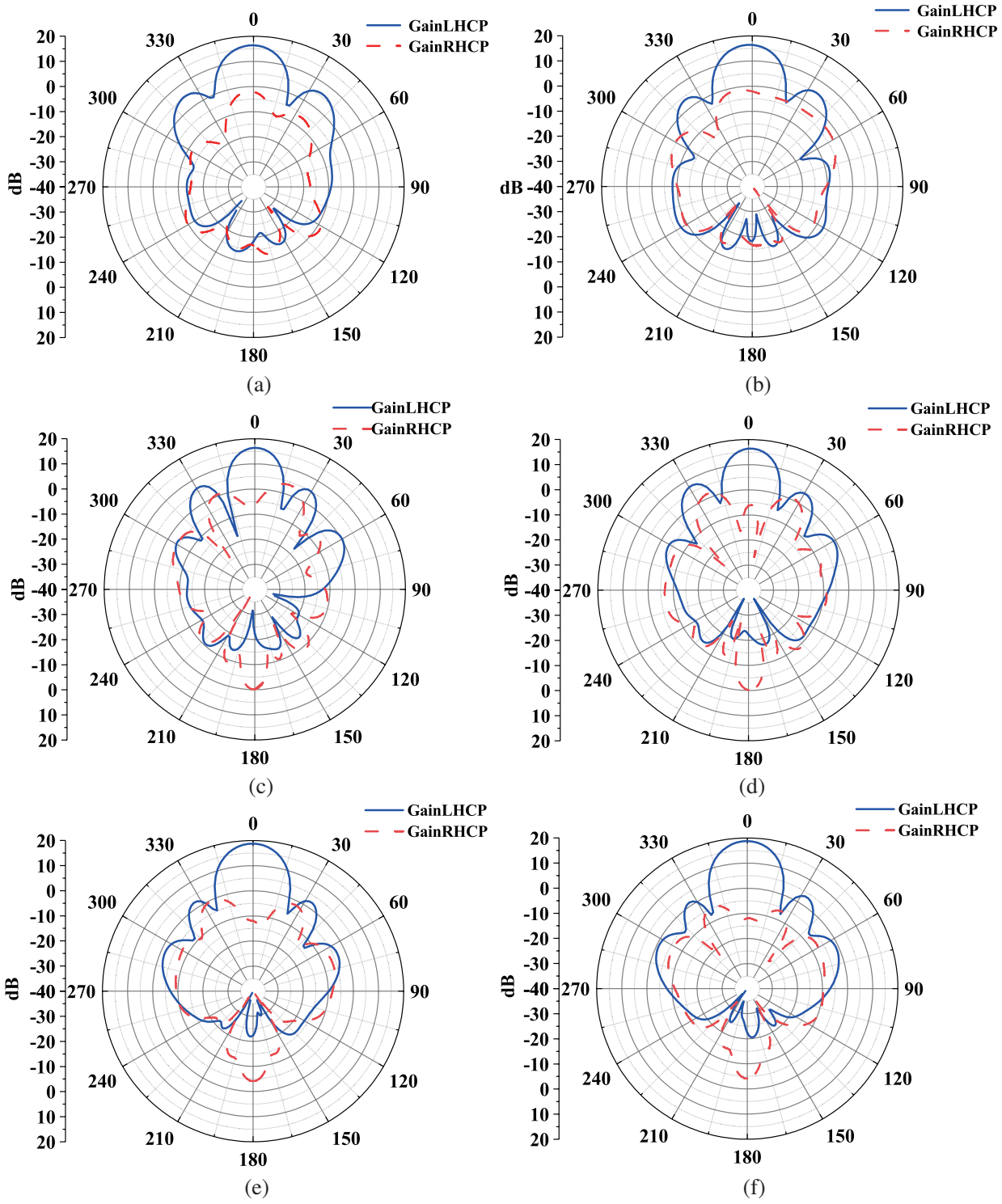

Figure 8. Plot of the polarization direction at 2.7 GHz, 3 GHz, 3.3 GHz. (a) 2.7 GHz-*xoz*, (b) 2.7 GHz-*yoz*, (c) 3 GHz-*xoz*, (d) 3 GHz-*yoz*, (e) 3.3 GHz-*xoz*, (f) 3.3 GHz-*yoz*.

guide structure reduces the loss and increases the gain. However, the frequency band in this paper is relatively low, and the SIW structure is not required. The use of the slot structure in [19] has a great impact on the axial ratio bandwidth and impedance bandwidth, both of which are relatively wide, but

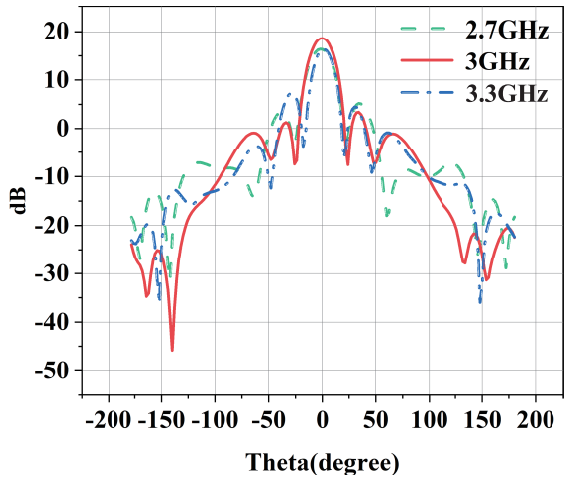

Figure 9. Gain at 2.7 GHz, 3 GHz, 3.3 GHz.

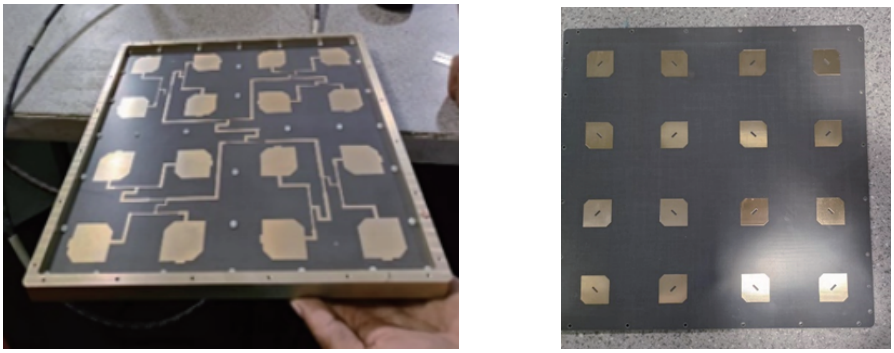

(a) (b)

Figure 10. Physical diagram of the antenna, (a) bottom, (b) leaded patch.

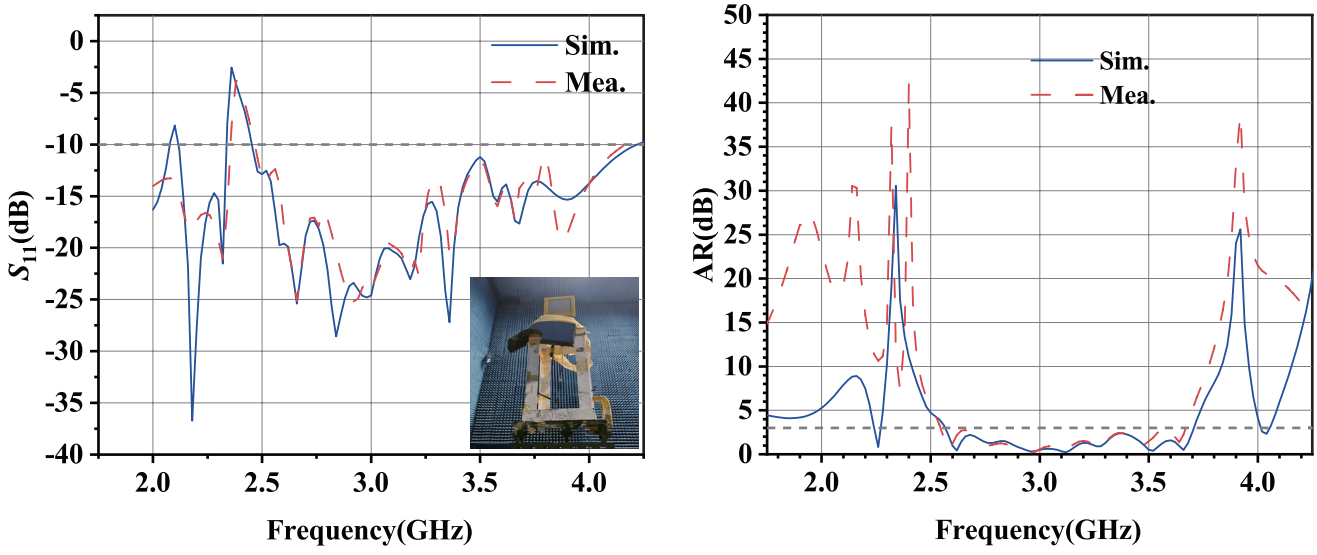

(a) (b)

Figure 11. Simulation and measurement of the S_{11} and AR. (a) S_{11}. (b) AR.

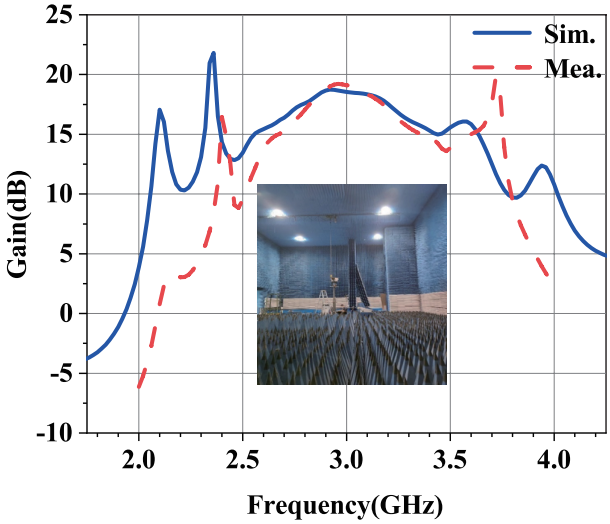

Figure 12. Simulation and measurement of gain.

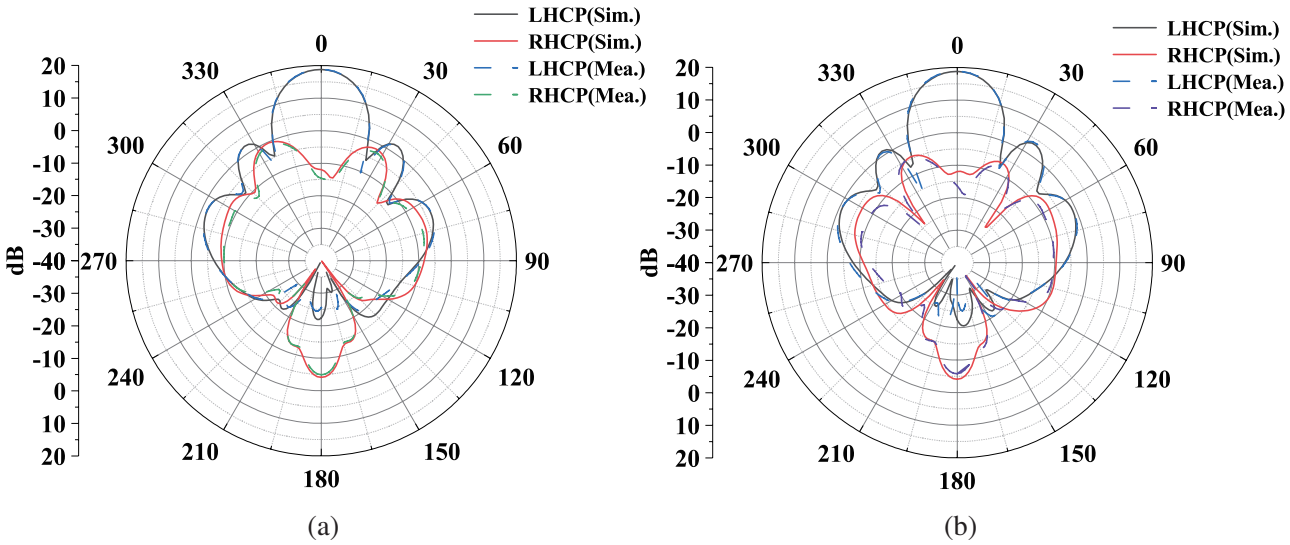

Figure 13. Simulation and measurement of the directional map at 3 GHz. (a) *xoz*, (b) *yoz*.

Table 2. Comparison of the literature.

Reference	Impedance bandwidth %	Axial ratio bandwidth %	Peak Gain
REF [17]	21.7	8.9	17.9 dB
REF [14]	24	20.6	11.8 dB
REF [15]	29	15.5	8.25 dB
REF [18]	20.8	18.3	20.3 dB
REF [19]	88.6	81.3	10.8 dB
REF [21]	14.7	14.7	17.2 dB
REF [22]	46	46	12.2 dB
REF [23]	12.5	14.7	12 dB
Proposed	51.5	38.2	18.72 dB

the antenna gain is general, and the pattern radiation has some offset, which is not very symmetrical. The maximum radiation direction is not at 0°. However, the pattern in this paper is very symmetrical at the center frequency, and the pattern has no offset, which can be widely used in practice. In [22], the axial ratio bandwidth is better, but the gain is lower than this paper.

4. CONCLUSION

In this paper, a CP antenna array with sequentially rotating feeds is proposed. The formation of the antenna is from the design of a basic antenna unit and power divider to the antenna array after combination. After simulation and measurement, the impedance bandwidth and axial ratio bandwidth of the antenna are good, and the peak gain is above 18 dB. The designed antenna not only satisfies the high gain but also solves the problem of the narrow bandwidth of the microstrip antenna. The antenna radiation pattern is stable, and the backward radiation is small, which can be applied in the actual radar system and 5G.

ACKNOWLEDGMENT

This work was supported by the Applied Basic Research of Liaoning Province (2022JH2/101300275) and the National Natural Science Foundation of China (61701211).

REFERENCES

1. Kraus, J. D. and R. J. Marhefka, *Antennae*, Electronic Industry Press, Beijing, 2011.
2. Grieg, D. D. and H. F. Engelmann, "Microstrip — A new transmission technique for the kilomegacycle range," *Proceedings of the IRE*, Vol. 40, No. 12, 1644–1650, 1952.
3. Zhong, S.-S., *Antenna theory and technology*, Electronic Industry Press, Beijing, 2015.
4. Byron, E. V., "A new flush-mounted antenna for phased-array applications," *Phased-Array Antenna Symp. Digest*, 187–192, 1970.
5. Xu, Y., L. Zhu, and N.-W. Liu, "Design approach for a dual-band circularly polarized slot antenna with flexible frequency ratio and similar in-band gain," *IEEE Antennas and Wireless Propagation Letters,*, Vol. 21, No. 5, 1037–1041, 2022.
6. Liu, N.-W., L. Zhu, Z.-X. Liu, Z.-Y. Zhang, and G. Fu, "Frequency-ratio reduction of a low-profile dual-band dual-circularly polarized patch antenna under triple resonance," *IEEE Antennas and Wireless Propagation Letters*, Vol. 19, No. 10, 1689–1693, 2020.
7. Liu, Y., et al., "A K-band broadband circularly polarized slot antenna based on L-shaped waveguide cavity," *IEEE Antennas and Wireless Propagation Letters*, Vol. 20, No. 9, 1606–1610, 2021.
8. Chandu, D. S. and S. S. Karthikeyan, "Broadband circularly polarized printed monopole antenna with protruded L-shaped and inverted L-shaped strips," *Microwave and Optical Technology Letters*, Vol. 1, No. 60, 242–248, 2018.
9. Yu, H.-Y., J. Yu, Y. Yao, X. Liu, and X. Chen, "Wideband circularly polarized horn antenna exploiting open slotted end structure," *IEEE Antennas and Wireless Propagation Letters*, Vol. 19, No. 2, 267–271, 2020.
10. Li, G. and F.-S. Zhang, "A compact broadband and wide beam circularly polarized antenna with shorted vertical plates," *IEEE Access*, Vol. 7, 90916–90921, 2019.
11. Qin, Y., X. Mo, R. Li, T. Wong, and Y. Cui, "A broadband wide-beam circularly polarized antenna array for urban macrocell base stations," *IEEE Transactions on Antennas and Propagation*, Vol. 67, No. 5, 3478–3483, 2019.
12. Hao, S.-S., Q.-Q. Chen, J.-Y. Li, and J. Xie, "A high-gain circularly polarized slotted patch antenna," *IEEE Antennas and Wireless Propagation Letters*, Vol. 19, No. 6, 1022–1026, 2020.
13. Leszkowska, L., M. Rzymowski, K. Nyka, and L. Kulas, "High-gain compact circularly polarized X-band superstrate antenna for cubesat applications," *IEEE Antennas and Wireless Propagation Letters*, Vol. 20, No. 11, 2090–2094, 2021.

14. Nasimuddin, X. Qing, and Z. N. Chen, "A wideband circularly polarized microstrip array antenna at Ka-band," *2016 10th European Conference on Antennas and Propagation (EuCAP)*, 1–4, 2016.
15. Maddio, S., "A compact wideband circularly polarized antenna array for C-band applications," *IEEE Antennas and Wireless Propagation Letters*, Vol. 14, 1081–1084, 2015.
16. Ta, S. X. and I. Park, "Compact wideband circularly polarized patch antenna array using metasurface," *IEEE Antennas and Wireless Propagation Letters*, Vol. 16, 1932–1936, 2017.
17. Lang, Y., S.-W. Qu, and J.-X. Chen, "Wideband circularly polarized substrate integrated cavity-backed antenna array," *IEEE Antennas and Wireless Propagation Letters*, Vol. 13, 1513–1516, 2014.
18. Hassan, A. T. and A. A. Kishk, "Circularly polarized antenna array based on microstrip ridge gap waveguide at 60 GHz," *2020 14th European Conference on Antennas and Propagation (EuCAP)*, 1–4, 2020.
19. Wang, H., J. Li, and L. Hao, "A broadband circularly polarized antenna array for wireless communication applications," *Radio Communication Technology Radio Communication Technology*, Vol. 01, No. 48, 180–187, 2022.
20. Li, M., *HFSS Antenna Design*, Electronic Industry Press, Beijing, 2011.
21. Kim, H., Y. Lee, and B. Kim, "60 GHz digitally controllable and sequentially rotated fed antenna array," *Electronics Letters*, Vol. 53, No. 13, 821–822, 2017.
22. Zhang, Z. and S. Zuo, "Broadband circularly polarized bowtie antenna array using sequentially rotated technique," *IEEE Access*, Vol. 6, 12769–12774, 2018.
23. Shen, Y., S. Zhou, and G. Huang, "A compact dual circularly polarized microstrip patch array with interlaced sequentially rotated feed," *IEEE Transactions on Antennas and Propagation*, Vol. 64, No. 11, 4933–4936, 2016.